Iranian Journal of Chemical Engineering
Vol. 16, No. 4 (2019), IAChE

Cooling Enhancement of a Photovoltaic Panel Through Ferrofluid Stimulation Using a Magnetic-Wind Turbine

N. Heidari [1], ***M. Rahimi*** [2*], ***N. Azimi*** [1]

[1] *Department of Chemical Engineering, Kermanshah Branch, Islamic Azad University, Kermanshah, Iran*
[2] *CFD Research Center, Department of Chemical Engineering, Razi University, Kermanshah, Iran*

ARTICLE INFO

Article history:
Received: 2019-11-12
Accepted: 2020-02-17

Keywords:
Heat Transfer,
Photovoltaic Panel,
Cooling,
Ferrofluid,
Magnetic Field

ABSTRACT

Wind energy is used to rotate a magnetic turbine in order to remove heat from the surface of a photovoltaic (PV) panel. A three-bladed turbine, which rotates with wind energy, has rotational motion underneath the studied PV panel in order to move Magnetic Nano-Particles (MNPs). In addition, effects of the magnetic field strength (B=450-830 mT), rotational velocity of the magnetic turbine (ω), and the concentration of MNPs (ϕ) on the heat removal from the PV panel area were investigated. Results showed that heat removal from PV panel was intensified by motion of pinned MNPs in the ferrofluid via the exerted external force of magnetic field. Concurrent application of available magnetic field along with ferrofluid led to 7.6-24 % temperature reduction for a PV panel. Furthermore, the produced electrical energy of the PV panel was augmented between 2.55-3.13 W depending on ϕ, ω, and B. Moreover, the impact of ω on cooling performance was also investigated, and a significant enhancement to generated power was observed. Eventually, the maximum amount of the produced power (3.13 W), maximum power enhancement percentage (32.63 %), and thermal efficiency (24 %) were achieved for B=830 mT, ω=50 cycles/min, and ϕ=0.05 (w/v).

1. Introduction

Nowadays, among the most essential resources of renewable energy, solar energy has gained much attention due to its free charge and permananet availablity [1-3]. Electricity can be produced via photovoltaic (PV) solar cells by transforming the photons attained through the sun into electrical energy [4, 5]. According to the literature [6, 7], close to 15 % of the existing solar power is transformed to electricity during the PV panel functioning, and the rest turns to heat. Thus, the absorbed heat energy causes an increase in the PV panel temperature and it subsequently leads to a reduction in the electrical conversion efficiency by 0.45 % with a 1 °C rise of the operational temperature [6-8]. Chow et al. [9] showed that a 10 °C increase in the surface temperature of PV panels led to a 5 % electrical efficiency reduction. This problem can be resolved by cooling and heat dissipation from PV surface during its operation [10-12]. To date, several technologies such as air-cooling [13], liquid

[*]Corresponding author: masoudrahimi@yahoo.com

immersion cooling [14], impingement/micro-channel [15], and nanofluid [16] were considered by authors to cool the PV panels. In addition, many experimental and theoretical works were completed by substituting the working fluid of the PV systems with nanofluids as coolant [1, 4-7, 16-24]. Sardarabadi et al. [5] numerically and experimentally checked the ability of TiO_2, Al_2O_3, and ZnO/ water nanofluids for cooling the Photovoltaic Thermal Unit (PVT). Results depicted that ZnO/ water and TiO_2/ water nanofluids enjoyed greater electrical efficiency than Al_2O_3/ water nanofluid and pure deionized-water.

Likewise, Karami et al. [16] estimated the cooling efficiency of a PV panel utilizing water-based nanofluids including nanoparticles of Boehmite. Attained results demonstrated that consuming nanofluid as operating fluid in considered PV led to a greater temperature reduction and had positive influence on its cooling efficiency. In addition, Khanjari et al. [17] numerically calculated the effects of various nanofluids applied to cooling a PV thermal system. They represented that by using alumina/water and Ag/water nanofluids, the maximum increase percentages of the cooling performance of the PV panel were 43 % and 12 %, respectively. Besides, Radwan et al. [18] applied SiC/water and Al_2O_3/ water nanofluids with various concentrations as cooling media in a photovoltaic thermal system and achieved greater electrical efficiency particularly at higher volume fraction of the nanoparticles and lower Reynolds number (Re). Hussien et al. [20] examined the applicability of a hybrid Photovoltaic/Thermal process (PV/T) by means of nanofluid as operational fluid. The achieved results indicated that utilizing nanofluid as coolant caused operating temperature reduction of PV panel. Additionally, Al-Waeli et al. [21] applied the SiC/water nanofluid as coolant for a PV/T system. Their results showed that while the concentration of SiC nanofluid was 3 wt %, the electrical efficiency and the thermal efficiency increased up to 24.1 % and 100.19 %, respectively, compared to use of water as coolant. Later, Sardarabadi et al. [23] elucidated the effects of simultaneous application of a Phase Change Material (PCM) and ZnO/water nanofluid as coolant media for a photovoltaic module. It was observed that the application of nanofluid enhanced the average thermal output by nearly 5 % for the PVT system. Yazdanifard et al. [24] gathered a valuable review of using nanofluid for cooling photovoltaic/thermal systems. They evaluated the effective parameters of the PVT system cooling performance. The attained outcomes depicted that in comparison with turbulent flow regime, nanofluids were more efficient for the laminar flow regime. Likewise, they indicated that although applying nanoparticles with large size to the turbulent regime caused greater exergy and energy efficiency, they exhibited different behaviors in laminar flow. From these reports, it can be concluded that using nanofluids for the PV panels could successfully enhance the cooling performance. The suspended nanoparticles are able to improve the heat transfer and thermal conductivity performance. However, a suitable and most effective selection of nanofluid is a key subject for PV panels cooling. The cooling efficiency of nanofluids in PV panels depends mainly on the shape, size, and category of nanoparticles, concentration and stability of nanofluid, and properties and temperature of base fluid [25]. Generally, the above reviewed papers focus

on the cooling performance improvement of PV systems using nanofluids and they only act as working fluids with high thermal conductivity, and not as mixing and turbulent agents. Besides, ferrofluids are one type of nanofluids containing magnetic nanoparticles suspended in a carrier liquid [26, 27]. Ferrofluids are introduced as an innovative agent to raise the convective flow and heat transfer in fluid when they are stimulated by an external Magnetic Field (MF) [28, 29]. Research studies on the application of ferrofluid to cooling of PV systems are quite limited in scope in the literature. In this context, Ghadiri et al. [7] proposed application of Fe_3O_4 water-based ferrofluid as coolant under constant and alternating magnetic fields in the cooling section to enhance the overall efficiency of a PVT. Their experimental results depicted that by using 3 wt % ferrofluid, the overall efficiency of the system was enhanced by 45 %, compared to that of the distilled water as coolant.

In this research, an experimental study is carried out to consider the effect of moving magnetic field on the heat removal and improving the cooling performance of a PV module. The novelty of this work is using wind energy that is free and available to rotate a three-bladed magnetic turbine to induce mixing in the ferrofluid and remove heat from the PV panel surface. The measured results of surface temperature, maximum power improvement, and electrical efficiency of a PV panel are reported. The layout of using pure-distilled water is selected as a reference for comparison with layout of using ferrofluid.

2. Experimental

2.1. Experimental setup and apparatus

The key constituents of the fabricated setup are PV panel, a three-bladed turbine, data attainment system, and solar simulator. Additionally, a mono-crystalline silicon photovoltaic panel (ZT10-18-P, ACDC, Taiwan) consists of 72 cells linked in series and parallel form with an active surface of 24 mm × 36 mm. The PV panel is located over a steel frame. Moreover, 12 thermocouples are joined on the PV panel area, with an enormously thin substrate of thermal epoxy in order to measure the temperature of PV panel. Fig. 1 shows the graphical scheme of a PV panel and the position of thermocouples.

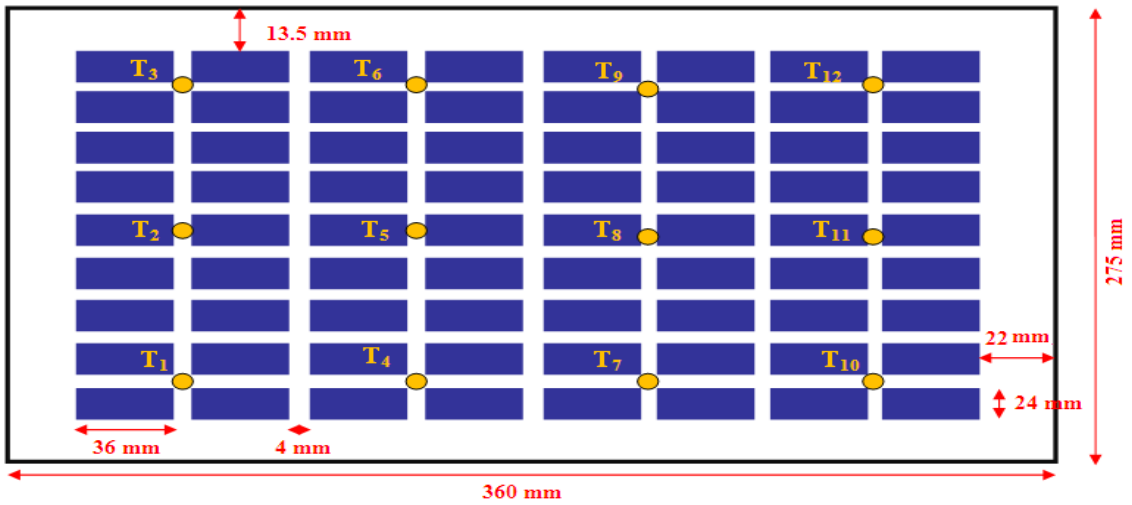

Figure 1. The scheme of the PV module and the thermocouple positions.

A graphical layout of experimental setup is clarified in Fig. 2. As seen in this figure, the exerted system containing a PV panel, data achievement system, solar simulator, test section, and a three-bladed turbine with three permanent magnets is attached to each blade.

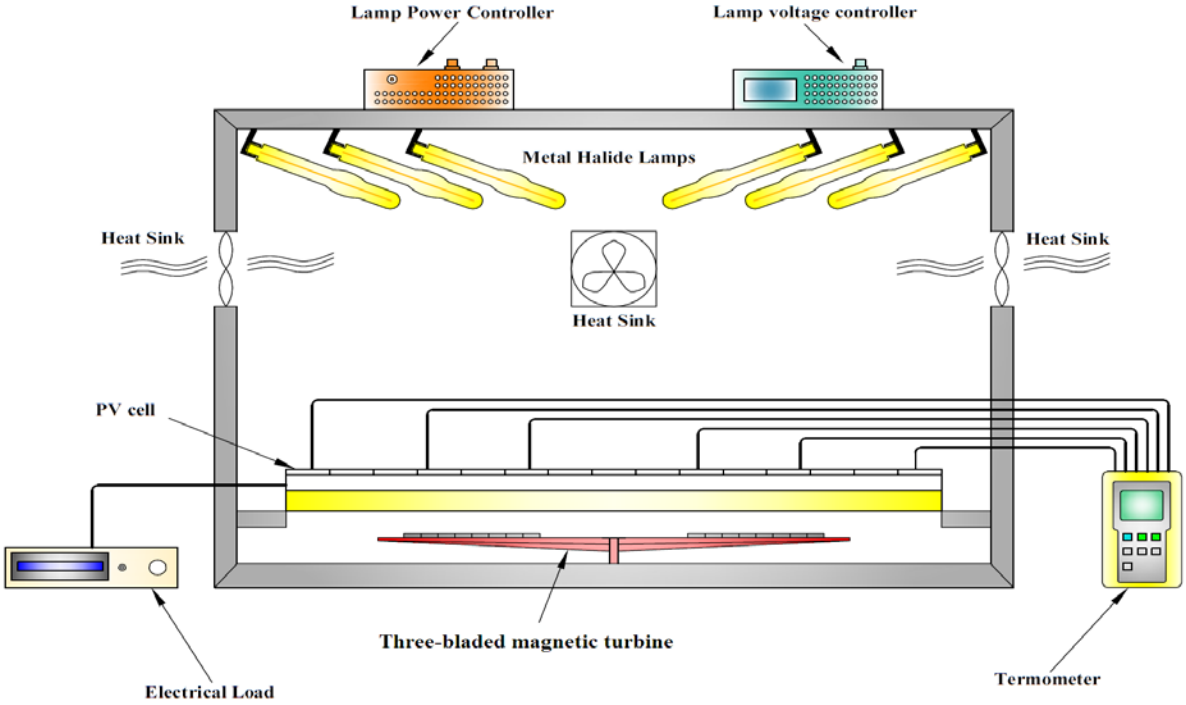

(2-D)

(3-D)

Figure 2. A schematic diagram of the experimental setup used in the present study.

A real photograph of three-bladed magnetic turbine is shown in Fig. 3. Three cubic permanent magnets (20 mm×50 mm×5 mm) are attached to the three-bladed turbine, and this set is moved by wind energy under the backside of the PV panel to create a mobile magnetic field.

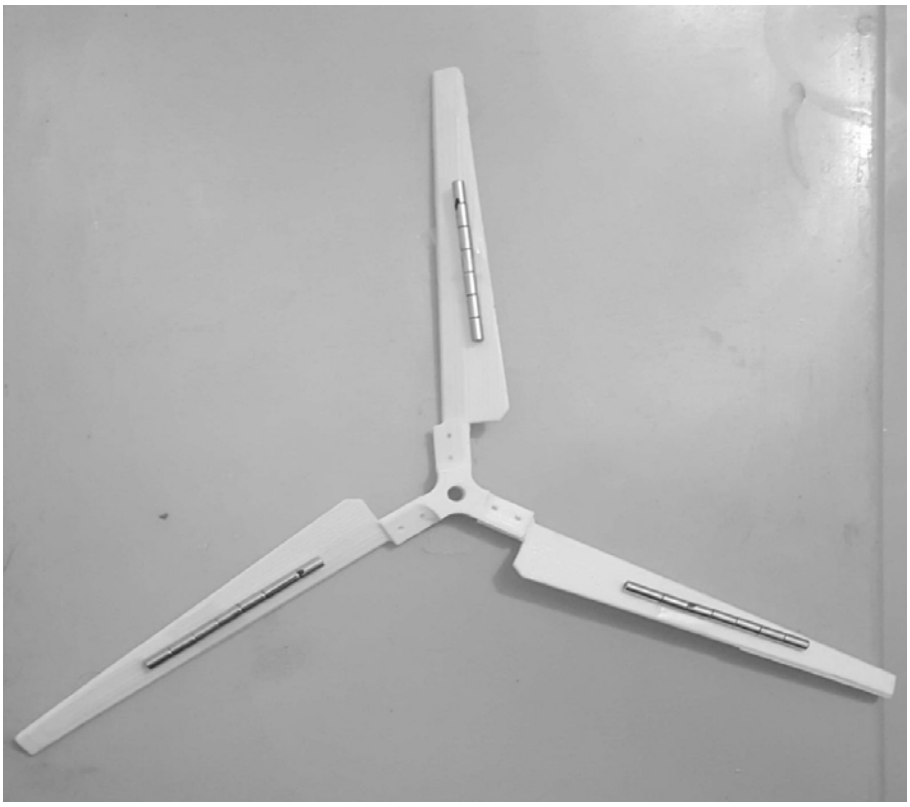

Figure 3. A real photograph of three-bladed magnetic turbine.

Indeed, Moving Magnetic Field (MMF) is induced by connecting three permanent magnets to the three-bladed turbine and has rotational motion using the wind energy. Likewise, to evaluate the effect of MMF, the rotational velocity of turbine is fixed at 15, 20, 30, 40, and 50 rad/s. It is essential to note that the magnetic field and magnetization direction (z-direction) are perpendicular to the surface of the PV module (x-direction). The strength of magnetic field (B) is controlled via changing the magnets distance from the PV panel surface and it is quantified through a digital TESLA meter with precision superior than 0.1 %. Besides, the distance (d) is adjusted to 2, 4, 6, 8, and 10 mm corresponding to B = 830, 720, 640, 530 and 450 mT, respectively.

The temperature measurement system and an electrical load system that connected to the PV electrical output are used to measure and record data. A Lutron, BTM-4208SD thermometer is utilized for temperature recording of 12 points in the PV panel external surface. The average amount of 12 evaluated temperatures is employed as the PV panel temperature. In order to provide the required solar irradiation, solar simulator is used. The primary idea to design a solar simulator was extracted from other literature [30, 31]. The solar simulator device contains 5 Metal Halide (MH) lamps located on an aluminum heat sink plane. The entering radiation intensity (I (W/m^2)) is quantified via a digital Pyranometer (Testo Company (Tes1333R)). In order to prepare the ferrofluid suspension, Fe_3O_4 nanoparticles with concentrations of 0.01, 0.02, 0.03, 0.04, and 0.05 (w/v) are well dispersed in distillated water as the reference liquid. Fe_3O_4 nanoparticles with a diameter less than 25 nm (purity, 99.5 %) used in this work are

supplied by US Research Nanomaterials Inc. (Houston, TX). The provided nano-suspension is made uniform using an ultrasonic homogenizer (Hielscher UP400S, Germany) to achieve a homogeneously dispersed system and prevent the Fe_3O_4 nanoparticles settlement. Hence, sonication process is performed at a frequency of 24 kHz and a nominal strength of 400 W. Within the sonication, nano-suspension temperature is controlled at 293–298 K such that the suspension vessel is bound via ice-water chilling bath. The elapsed time is 90 minutes to make ready a permanent/stable ferrofluid.

2.2. Test procedures

The reservoir of the PV panel is full of about 2 Liter of working fluid, which is in the batch state (working fluid does not have any flow). At the first stage, the reservoir is full of the pure-distilled water, and the solar simulator lamps are turned on. Simultaneously, the temperatures of 12 places on the PV panel area are listed using the thermometer. The radiation power is set to 1000 W/m^2 during the tests. The tests are completed at ambient temperature (17 °C). Furthermore, to specify the amounts of current I (I_{max} in A), the maximum power point (P_{max}) and voltage V (V_{max} in V) at maximum intensity of the PV panel, I–V quantities are registered untill the system achieves a steady-state condition. Subsequently, this method is also used for ferrofluid with concentrations of 0.01, 0.02, 0.03, 0.04, and 0.05 (w/v). In order to confirm repeatable and reliable results, the experiments are conducted three times.

3. Uncertainties analysis

The measurement apparatuses used in this task are calibrated, and the uncertainty examination is well defined. Evaluated data is summarized as "the evaluated value ± uncertainty''. The subsequent computations are utilized for this aim:

$$\bar{x} = \frac{1}{N}\sum_{i=1}^{N} x_i \tag{1}$$

$$\sigma_x = \sqrt{\frac{1}{N-1}\sum_{i=1}^{N}(x_i - \bar{x})^2} \tag{2}$$

where N is the number of measured values, $\bar{x}$ is average measured quantities, x is the quantity, and σ_x is the standard deviation. The evaluated quantities are listed as $x = \bar{x} \pm RDS\,(\%)$ or $x = \bar{x} \pm \sigma_x$.

Here, RSD stands for the relative standard deviation and is computed as follows:

$$RDS\,(\%) = 100\frac{\sigma_X}{\bar{x}} \tag{3}$$

The highest uncertainty of calculations is determined close to 4.1 % for the surface temperature of PV panel, 4.9 % for P, and 3.9 % for V.

4. Results and discussion

As it is explained in the experimental section (part 2.1), the temperatures of 12 places are recorded at PV panel surface in each 5 minutes until achieving a steady-state condition (after approximately 45 minutes). The average temperature of these 12 positions is calculated as the average temperature of the PV panel. Therefore, two working fluids are applied in this project: pure-distilled water and a ferrofluid (Fe_3O_4 water based) with five various volume concentrations (0.01-0.05 (w/v)). The ferrofluid is considered in two situations: the first one without the magnetic field and the second one in the presence of the magnetic field with permanent rotational motion of the magnets.

4.1. Average temperature of the PV panel in various layouts

Fig. 4 shows the average temperature variation of the PV panel at solar energy of 1000 W/m^2.

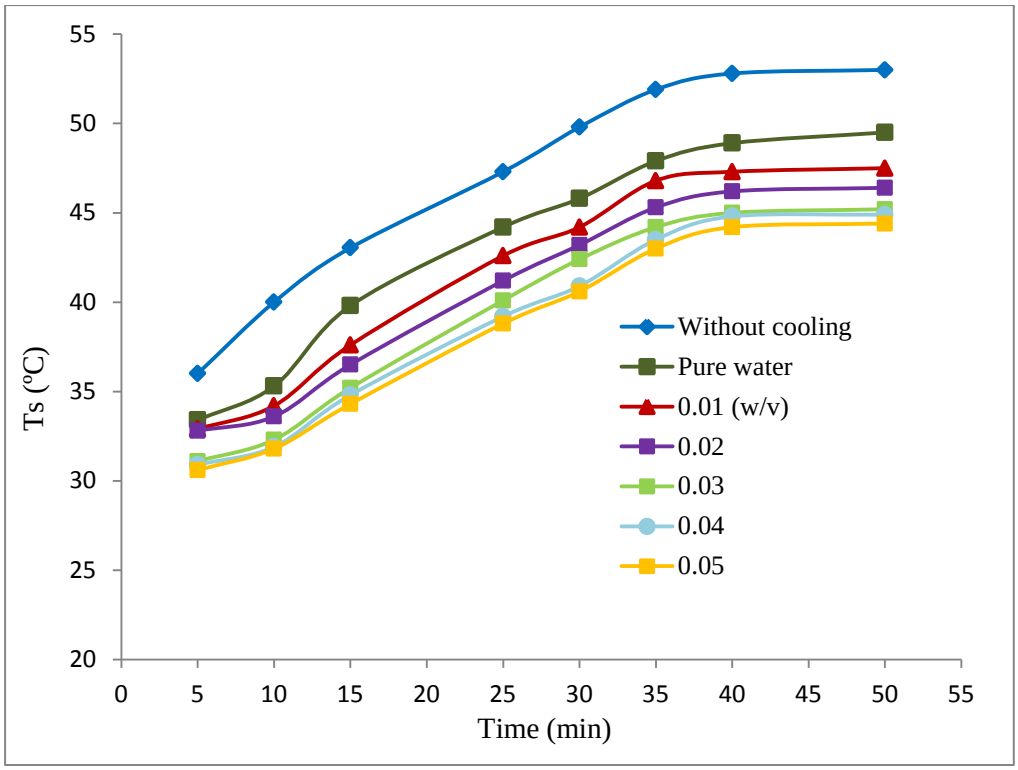

Figure 4. Variation in the average temperature of the PV module surface (T_s) for layouts without cooling and using pure water and ferrofluid as coolants.

Fig. 4 shows the results of three different layouts: without considering cooling apparatus (Case 1), pure-distilled water as a coolant fluid (Case 2), and ferrofluid usage without magnetic field at different concentrations of ferrofluid (Case 3). The system accomplishes the steady-state condition in 45 minutes and the average temperature of the panel surface reaches 52.6 °C. While pure water is used as a coolant fluid, the average surface temperature (T_s) ranges around 49.5 °C in the steady-state condition. According to the figures, the addition of ferro-nanoparticles to water solvent and without any magnetic field (for wholly considered concentration) T_s of the PV panel decreases. The presence of MNPs in the working fluid leads to nanoparticle assembling, Brownian motion, and viscosity changing obtained by the heat transfer augmentation in nanofluid [32-34]. Furthermore, adding MNPs to water causes the thermal conductivity improvement of nanofluid as well as the thermal boundary substrate destruction. In addition, adding MNPs to water causes increase in the thermal conductivity of the nanofluid along with the disturbed thermal boundary layer. From this figure, it can be concluded that the concentration of ferrofluid has a considerable role in decreasing T_s of the PV panel and in the decreasing trend for $T_{surface}$ can be seen for increasing ferrofluid concentration. This effect is more dominant for the ferrofluid with

the concentration of 0.01 to 0.04 (w/v) while increasing it from 0.04 to 0.05 (w/v) has no siginificant effect on decreasing T_s. It is observed that T_s for 0.04 and 0.05 (w/v) ferrofluid without magnetic field decreases to nearly 44.4-44.9 ºC, whereas, this amount for the cases without cooling and using pure-distilled water was about 52.6 °C and 49.5ºC, respectively.

4.2. Effect of magnetic field and ferrofluid concentration on PV panel temperature

Fig. 5 shows the mean temperature variation of the PV panel surface versus time for several concentrations of ferrofluid, while the magnetic field induction (B) is 830 mT and the magnet rotational velocity (ω) is about 30 rad/s.

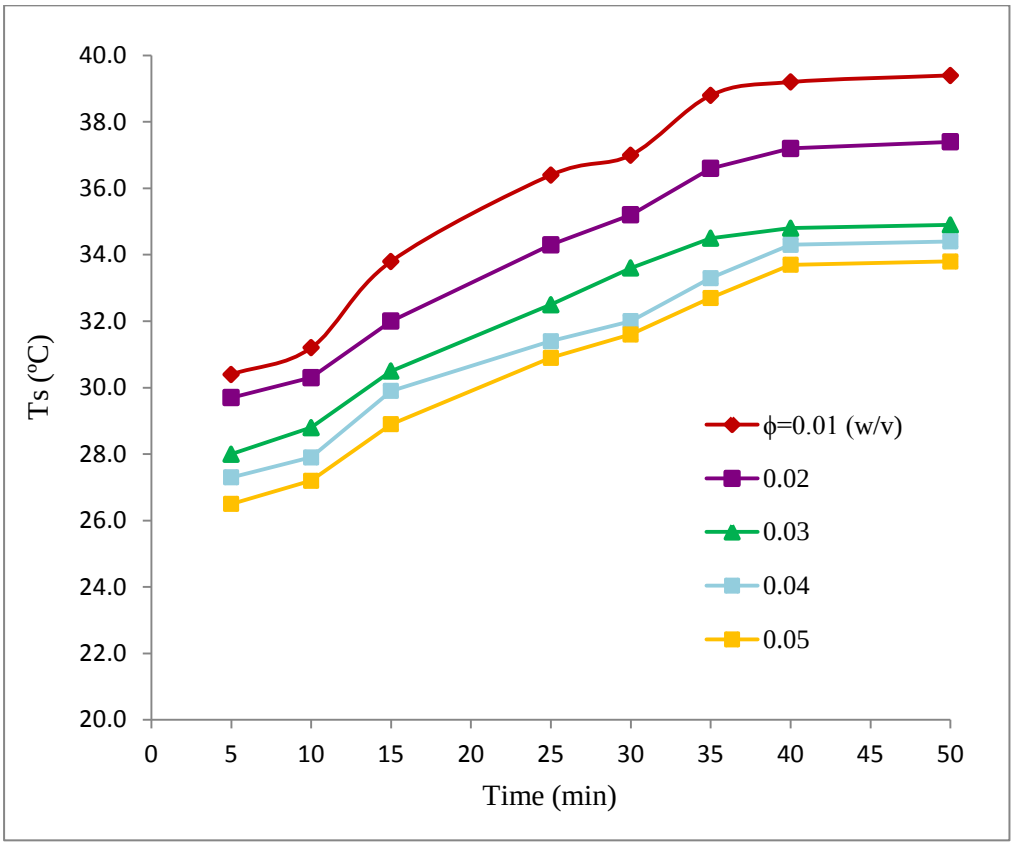

Figure 5. Variation in the average temperature of the PV module surface by time at different concentrations of ferrofluid fluid (B=830 mT, ω=30 rad/s).

Figs. 4 and 5 show that applying magnetic field to ferrofluid causes a further reduction in surface temperature of the studied PV panel. From Fig. 5, 0.01 (w/v) ferrofluid has the uppermost mean temperature in comparison with other concentrations, and its quantity in the steady-state condition reaches 39.4 °C. The mixture including 0.05 (w/v) of ferrofluid indicates smaller quantities of temperature (33.8 °C in the steady-state condition) and improved cooling efficiency. Increasing the concentration of MNPs from 0.04 (w/v) to 0.05 (w/v) does not have substantial effect on the surface temperature reduction of PV panel after attaining the steady-state condition.

However, as concentration of MNPs increases from φ= 0.04 (w/v) to φ= 0.05 (w/v), the temperature of the PV panel has no significant changes. Here, it should be expressed that increase in the ferrofluid

concentrations has two mutual effects: the positive effects are boosting the thermal conductivity and disturbance in thermal boundary layer, hence an increase in the heat transfer from the surface of the PV panel to the ferrofluid. The increase observed in the cooling performance of the PV panel by ferrofluid concentration under moving magnetic field is assumed to be associated with more intense disturbance in thermal boundary layer generated by chaotic and angular movement of MNPs. Contrarily, by increasing MNPs concentration (from 0.04 to 0.05 w/v), greater agglomeration/chaining of suspended magnetic nanoparticles can occur. An important challenge for nano/ferrofluids is that nanoparticles tend to accumulate due to molecular interactions such as Van der Waals forces. Therefore, as the nanoparticles concentration increases, their accumulation also increases. In addition, the fluid viscosity is increased and the thermal performance of the fluid decreases by decreasing the effective surface area to volume ratio. However, the confrontation of positive and negative effects is positive in the strong enough magnetic field.

Here, to enhance comprehension of magnetic field and ferrofluid concurrent effects on T_s reduction, the percentage of PV surface temperature reduction (T_s) in the case of applying magnetic field relative to its value without magnetic field (T_{s0}) (Fig.4) (% $T_{s\ \text{decrease}}$) is defined as follows:

$$\%T_{s\ \text{decrease}} = \left|\left(\frac{T_s - T_{s0}}{T_{s0}}\right)\right| \times 100 \qquad (4)$$

Fig. 6 shows % $T_{s\ \text{decrease}}$ at various ferrofluid volume concentrations. This figure obviously depicts that the magnetic field has positive effects on the cooling efficiency of the PV system.

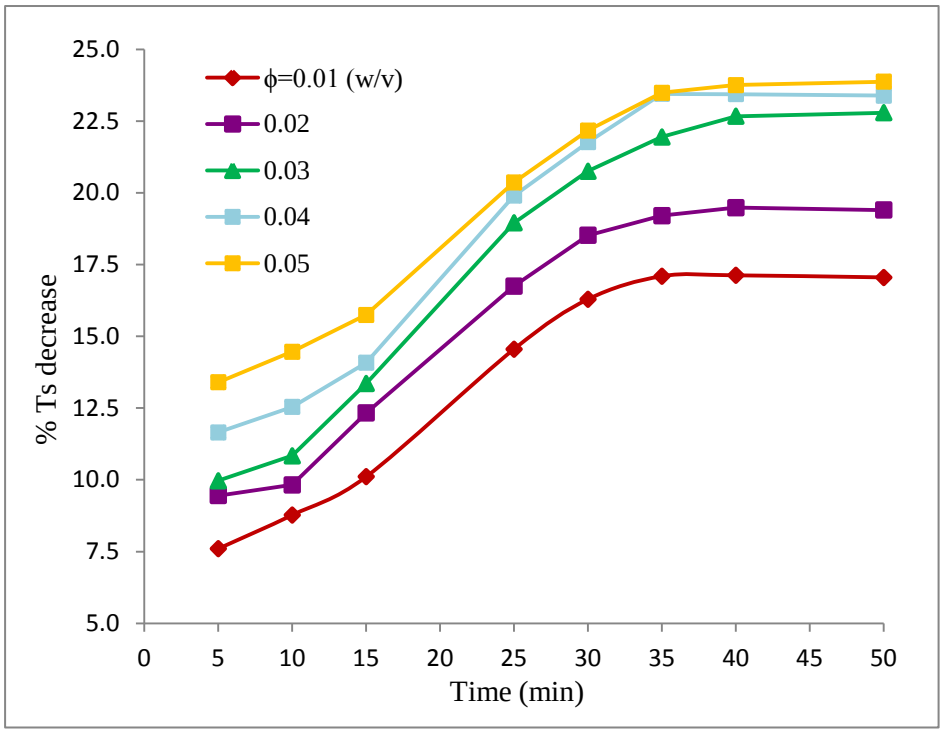

Figure 6. Variation of the efficiency of the PV temperature decrease under magnetic field (% $T_{s\ \text{decrease}}$) relative to ferrofluid without magnetic field for different concentrations of MNPs (B=830 mT, ω=30 rad/s).

Indeed, using a moving magnetic field with a magnetic field induction of 830 mT increases the % $T_{s\ decrease}$ by about 7.6 to 24.55 % in comparison with magnetic field elimination. This occurs due to chained MNPs motion and their cluster morphology. The motion and the body forces of external magnets cause the movement of pinned MNP clusters perpendicular to underneath the PV panel, leading to more heat transfer in this case [33, 34]. Evidently, the ferrofluid thermal efficiency is augmented by MNPs concentration increment, and the highest values are attributed to 0.05 (w/v) ferrofluid. The thermal efficiency value of 0.05 (w/v) ferrofluid is 3-5 times higher than those of 0.01 (w/v) ferrofluid.

4.3. Effect of B and ω on the PV panel temperature

In this work, magnetic field induction effect (B=830, 720, 640, 530, and 450 mT) on average temperature variation of the PV panel surface is studied. According to Fig. 7, the average temperature of the PV panel surface is low at high magnetic field induction and cooling efficiency is enhanced.

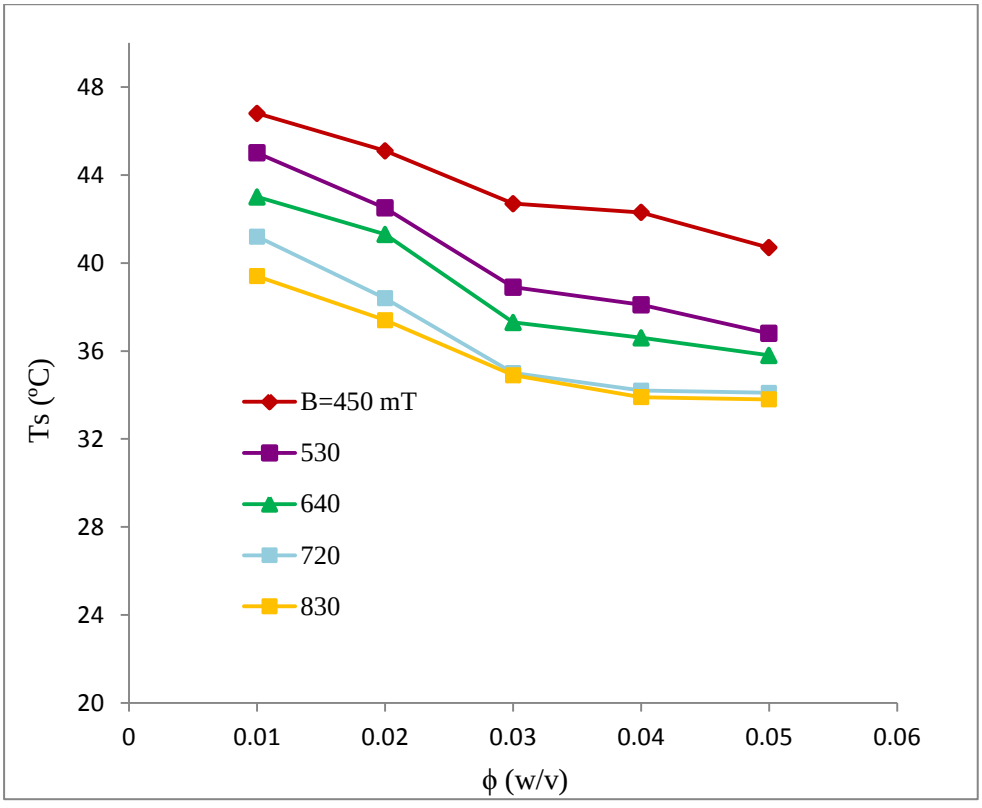

Figure 7. Variation in the average temperature of the PV module surface by concentrations of ferrofluid at magnetic field induction (ω=30 rad/s).

In this work, the effects of the magnetic field induction (B=830, 720, 640, 530, and 450 mT) on the variation in the average temperature of the PV module surface are studied. As it can be seen in Fig. 7, at high magnetic field induction, the average temperature of the PV panel shows lower values and cooling performance is enhanced. As presented in Fig. 7, the values of T_s increased with an increase in B and a significant effect as great as T_s value about 33.8 °C is achieved when B=830 mT and

ϕ=0.05 (w/v). The differences between T_s values for ϕ=0.03-0.05 (w/v) at B=720 and 830 mT are ignorable compared with those of other concentrations. Indeed, the external magnetic field has lower influences on heat transfer characteristics when magnetic field is strong enough to move the pinned MNPs or nanoparticles chains. However, the effect of magnet rotational motion (ω) should be investigated in order to select the efficient magnetic field induction. Therefore, ϕ=0.04 (w/v) is chosen as a selected ferrofluid concentration for subsequent experiments in Fig. 8.

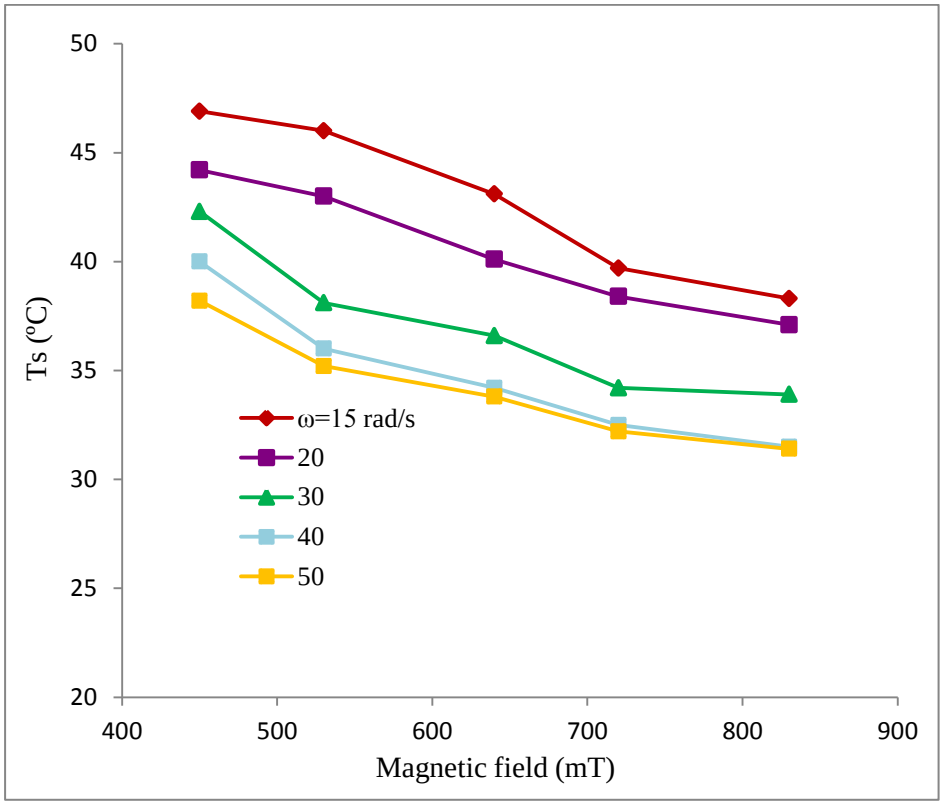

Figure 8. Variation in the average temperature of the PV module surface by magnetic field induction at different ω (ϕ=0.04 (w/v)).

In the later step, the effect of rotational speed of magnet (ω) is investigated while magnetic field induction is changed and ϕ is constant equal to 0.04 (w/v). Fig. 8 shows the obtained experimental dependences of the average temperature of the PV module surface values on ω under magnetic field. According to this figure, T_s decreased with increasing the rotational speed (ω). In this figure, it reached the minimum value (31.4 °C) at magnetic field induction about 830 and ω=50 rad/s. As described earlier, an external moving magnetic field causes nanoparticles to form chains that break and reform. It can induce intense motion of magnetic beads and thereby generate local vortices across the backside of the PV module. By increasing the rotational speed of magnet, the irregular motion of chains or pinned MNPs increases and it results in more intense local vortices and enhancement of the cooling performance. Therefore, the values of T_s with ω being 50 rad/s are lower than those of low rotational speeds (15, 20 and 30 rad/s)

under the same condition. In addition, Fig. 8 depicts that the values of T_s at ω=40 rad/s are very close to those of ω=50 rad/s. This means that applying moving magnetic field and rotation of MNPs chains in the fast enough rotational speed (40 rad/s) could solve the problem of poor mixing and heat transfer seen at lower rotational speeds (15, 20, and 30 rad/s). However, by increasing the rotational speed of magnetic turbine from ω=40 rad/s to ω=50 rad/s, only the energy is consumed. This means that ω=40 rad/s is fast enough to rotate the nanoparticle chains. Therefore, ϕ=0.04 (w/v) and ω=40 rad/s are chosen as the selected layouts for subsequent experiments in later section.

4.4. Panel electrical efficiency

To investigate the effect of cooling process on produced electricity using PV panel, the PV panel efficiency was measured in various situations. Then, the V–I information was recorded from the tests at five various magnetic field inductions for ω=40 rad/s and the concentration of 0.04 (w/v). The experimental I–V features of solar system over the varieties of normal local time without cooling apparatus and as an example for 0.04 (w/v) of ferrofluid are plotted in Fig. 9.

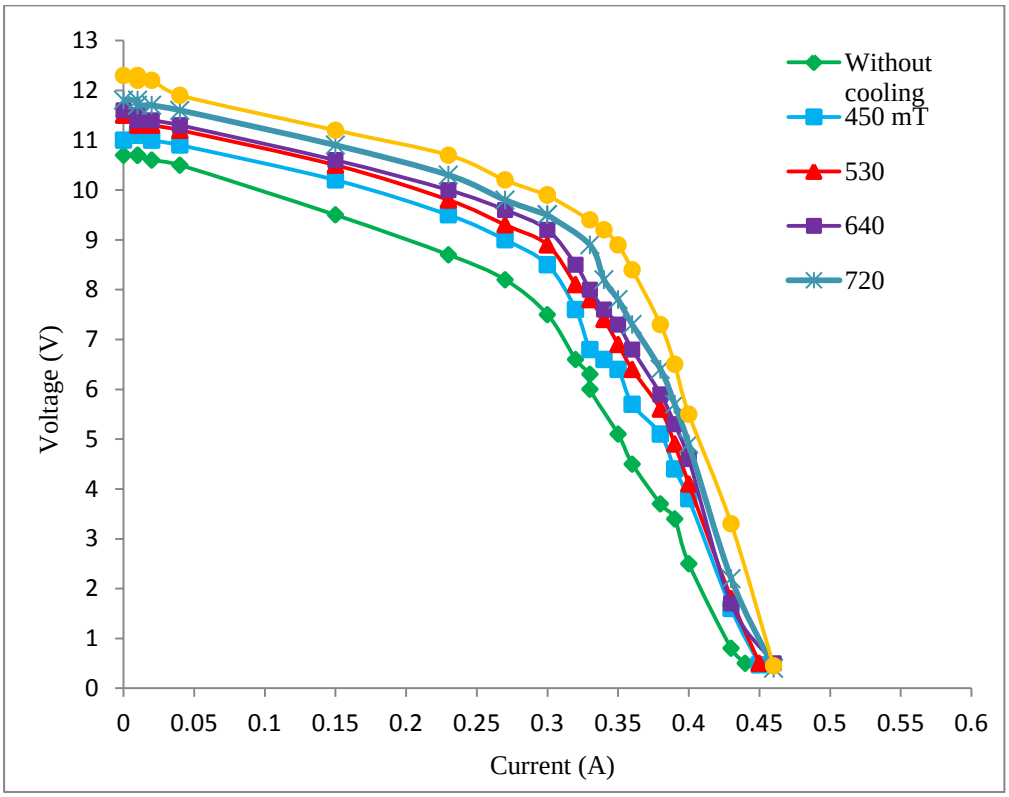

Figure 9. Current–voltage characteristic for 0.04 (w/v) ferrofluid at different magnetic field inductions (ω=40 rad/s).

Since the area under the I–V curve depicts the generated electrical power, the comparison between obtained results shows an increase in output power by stimulation of ferrofluid by magnetic field in the PV module. Furthermore, elimination of cooling system layout is compared with ferrofluid utilization as a coolant fluid under magnetic field, and it is observed that for the item of ferrofluid usage as an operational fluid, the

downward area of the I–V curve is higher than that of no cooling system layout for all quantities of magnetic field inductions. As it can be visibly understood, the downward area of the I–V curve increases with magnetic field induction. It could highlight the effect of simultaneous use of ferrofluid and moving magnetic field on the performance of the PV module better. Therefore, it is essential to describe and compute the produced power from the PV panel as follows:

$$P_{PV} = I_{PV} \times V_{PV} \quad (5)$$

where V and I are current intensity and voltage, respectively. The produced power of PV panel cooled with 0.04 (w/v) ferrofluid and ω=40 rad/s is schemed as a function of vent voltage in Fig. 10.

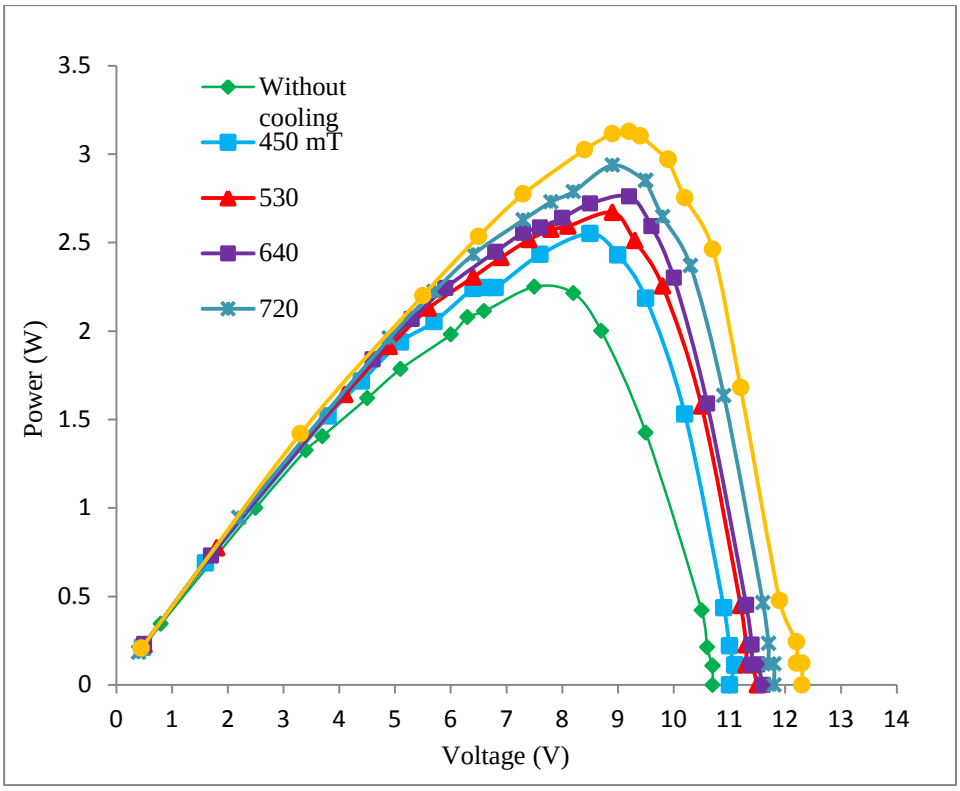

Figure 10. Maximum generated power from the PV cell for 0.04 (w/v) ferrofluid at different magnetic field inductions (ω=40 rad/s).

Evidently, the generated power of the PV panel increases as the magnetic field induction is augmented. As formerly stated, increasing the magnetic field induction leads to cooling efficiency increment of the PV panel and its temperature reduction; therefore, the produced power is enhanced owning to PV panel temperature reduction. Afterwards, the attained results of output power in the case of cooling system are compared with the presence of ferrofluid as a coolant fluid, and the impact of the magnetic field on the PV panel efficiency with ferrofluid as an operational fluid is noticeable. In addition, from Fig. 10, it can be concluded that for the layout of actuation of ferrofluid by magnetic field, the PV module achieves a maximum power output of 2.44 W, which is related to B=830 mT at a voltage of 7 V. A graphic schematic of the maximum produced power in the PV panel is designed in Fig. 11 at various concentrations of MNPs.

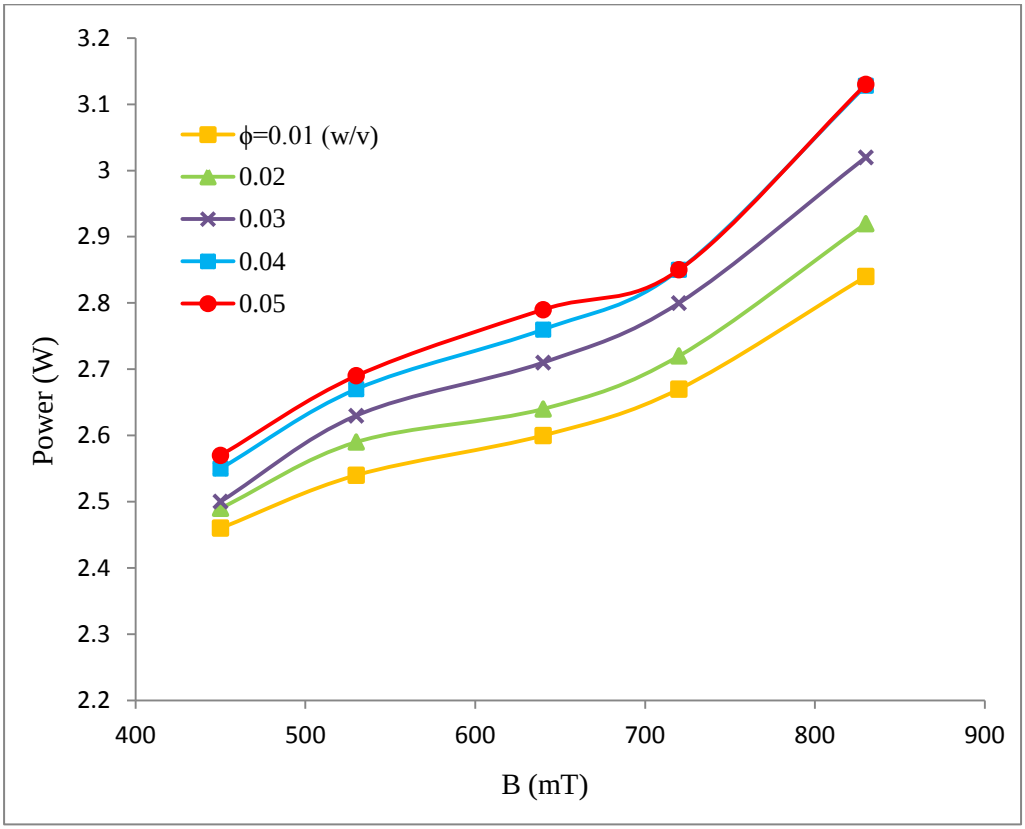

Figure 11. Maximum generated powers of the PV module by different magnetic field inductions at different concentrations of ferrofluid fluid (ω=40 rad/s).

Generally, this figure reveals that increasing the concentration of the ferrofluid under the magnetic field in the studied PV module produces remarkable amounts of electrical energy. In the studied range of 450-830 mT of the magnetic field induction, it is noticed that there is a trend from low to high values of generated power for all of the ferrofluid concentrations. For a better understanding of ferrofluid effect as a coolant fluid and magnetic field influence as an external force on the PV panel produced power, the percentage augmentation in electrical output PV panel is described as follows:

$$\%P_{(\max)increase} = \left(\frac{P_{ferrofluid} - P_{no\ cooling}}{P_{no\ cooling}}\right) \qquad (6)$$

Fig. 12 depicts the percentage increase in the electrical PV output for the different ferrofluid concentrations and at magnetic field inductions. The obtained results of ferrofluid concentration from 0.01 to 0.05 (w/v) show that by increasing MNPs concentration, the percentage of maximum power increases and raises remarkably at all of the magnetic field inductions. It can be seen that the higher electrical efficiency (32.63 %) is obtained with 0.05 (w/v) ferrofluid at B=830 mT, as the lowest average temperature of the PV module was detected in this layout. However, at a concentration higher than 0.04 (w/v) and magnetic field higher than 720 mT, the efficiency remains nearly constant, thus a greater increase in ferrofluid concentration has no significant effect on the percentage increase in the electrical PV output.

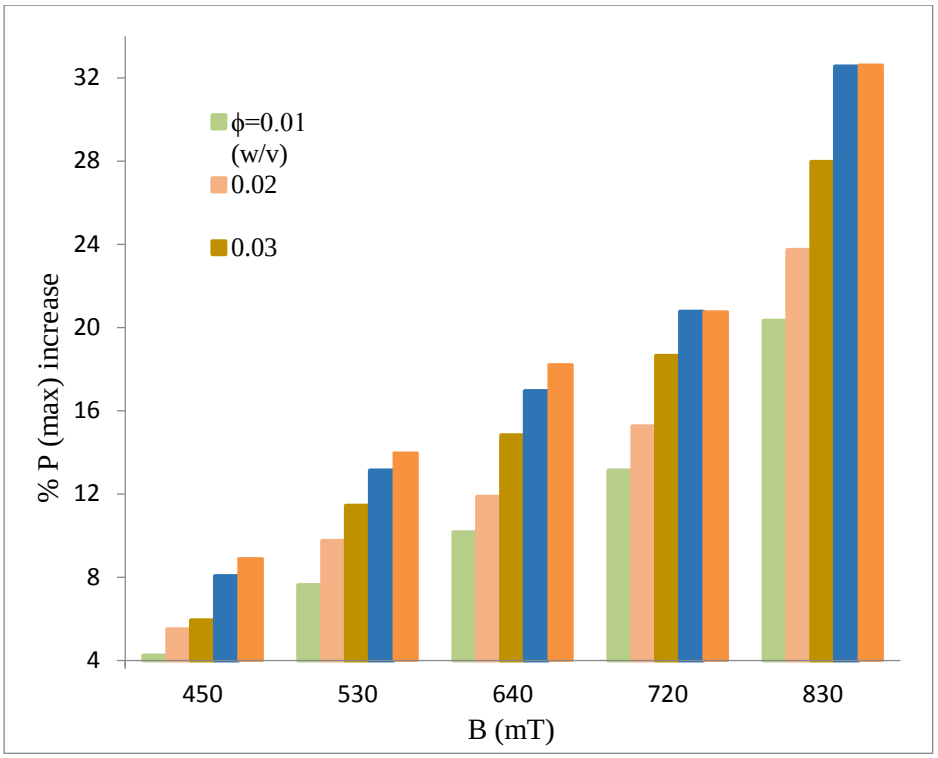

Figure 12. The percentage increase in the PV electrical output at different concentrations of ferrofluid.

5. Conclusions

This experimental research aimed to examine the effect of ferrofluid stimulation using a three-bladed magnetic turbine for cooling a PV panel. First, average surface temperature of the PV panel was recorded based on time without applying cooling system to achieve steady-state condition. Furthermore, the effect of using Fe_3O_4 ferrofluid (0.01-0.05 (w/v)) was experimentally investigated as an operational fluid stimulated using a moving magnetic field. Using magnetic field and ferrofluid as a functioning fluid, the thermal and electrical results of the systems were compared with pure-distilled water and utilizing ferrofluid without magnetic field. Results showed that stimulation of ferrofluid by moving magnetic field as a cooling method improved the cooling efficiency of the considered PV panel. Besides, results illustrated that magnetic nanoparticles actuation would significantly decrease the average surface temperature of PV panel compared to that without cooling system, pure water utilization as a working fluid, and ferrofluid application without magnetic field. Simultaneous use of ferrofluid and moving magnetic field exerted magnetic torque on MNPs along with fluid vorticity, which improved the heat transfer process. Motion of magnet on the backside of the PV module led to motion of pinned MNPs; thus, increasing the cooling efficiency from 7.6-24 % and the percentage of maximum power increase from 4.24-32.63 % were related to magnetic field induction (B) and the reciprocation speed of magnet motion (ω). The experiments performed in the course of this study revealed that using Fe_3O_4 ferrofluid stimulated by the three-bladed magnetic turbine that works with the wind energy significantly improved the thermal and electrical efficiency of the PV module.

Nomenclature

I	average intensity on absorber plate [W/m^2].
I_{PV}	photovoltaic arrays current [A].
P_{max}	maximum power of photovoltaic arrays [W].
$P_{ferrofluid}$	power of photovoltaic arrays by cooling with nanofluid [W].
P_{PV}	photovoltaic arrays power [W].
$P_{withoutcooling}$	reference power [W].
T_s	temperature of photovoltaic arrays using ferrofluid under magnetic field [°C].
T_{so}	temperature of photovoltaic arrays by using ferrofluid without magnetic field [°C].
V_{PV}	photovoltaic arrays voltage [v].
Subscripts	
max	maximum.
Abbreviations	
PV	photovoltaic.
MMF	moving magnetic field.

References

[1] Al-Waeli, A. H. A., Sopian, K., Chaichan, M. T., Kazem, H. A., Hasan, H. A. and Shamani, Al. N. A., "An experimental investigation of SiC nanofluid as a base-fluid for a photovoltaic thermal PV/T system", *Energy. Convers. Manage.*, **142** (15), 547 (2017).

[2] Kazem, H. A., Al-Badi, H. A. S., Al-Busaidi, A. S. and Chaichan. M. T., "Optimum design and evaluation of hybrid solar/wind/diesel power system for Masirah Island", *Environment, Develop. Sustain.*, **19** (5), 1761 (2017).

[3] Chandel, S. S. and Agarwal, T., "Review of cooling techniques using phase change materials for enhancing efficiency of photovoltaic power systems", *Renew. Sustain. Energy. Reviews*, **73**, 1342 (2017).

[4] Sardarabadi, M. Hosseinzadeh, M., Kazemian, A. and Passandideh-Fard, M., "Experimental investigation of the effects of using metal-oxides/water nanofluids on a photovoltaic thermal system (PVT) from energy and exergy viewpoints", *Energy*, **138** (1), 682 (2017).

[5] Sardarabadi, M. and Passandideh-Fard, M., "Experimental and numerical study of metal-oxides/water nanofluids as coolant in photovoltaic thermal systems (PVT)", *Sol. Energy Mater. Sol. Cells*, **157**, 533 (2016).

[6] Sardarabadi M., Passandideh-Fard M. and Zeinali Heris, S., "Experimental investigation of the effects of silica/water nanofluid on PV/T (photovoltaic thermal units)", *Energy*, **66** (1), 264 (2014).

[7] Ghadiri M., Sardarabadi, M., Pasandideh-fard, M. and Moghadam, A. J., "Experimental investigation of a PVT system performance using nano Ferrofluids", *Energy. Convers. Manage.*, **103**, 468 (2015).

[8] Kalogirou, S. A. and Tripanagnostopoulos, Y., "Hybrid PV/T solar systems for domestic hot water and electricity production", *Energy. Convers. Manage.*, **47** (18-19), 3368 (2006).

[9] Chow, T. T., Hand, J. W. and Strachan, P. A., "Building-integrated PV and thermal applications in a subtropical hotel building", *Appl. Therm. Eng.*, **23** (16), 2035 (2003).

[10] Karami, N. and Rahimi, M., "Heat transfer enhancement in a hybrid microchannel-photovoltaic cell using Boehmite nanofluid", *Int. Commun. Heat. Mass. Transfer*, **55**, 45 (2014).

[11] Han, X., Wang, Y. and Zhu, L., "The performance and long-term stability of silicon concen-trator solar cells immersed in dielectric liquids", *Energy.*

Convers. Manage., **66**, 189 (2013).

[12] Böer, K. W., "Cadmium sulfide enhances solar cell efficiency", *Energy. Convers. Manage.*, **52** (1), 426 (2011).

[13] Teo, H. G., Lee, P. S. and Hawlader, M. N. A., "An active cooling system for photovoltaic panels", *Appl. Energy.*, **90** (1), 309 (2012).

[14] Zhu, L., Wang, Y., Fang, Z., Sun, Y. and Huang, Q., "An effective heat dissipation method for densely packed solar cells under high concentrations", *Sol. Energy. Mater. Sol. Cells.*, **94** (2), 133 (2010).

[15] Barrau, J., Rosell, J., Chemisana, D., Tadrist, L. and Ibañez, M., "Effect of a hybrid jet impingement/micro-channel cooling device on the performance of densely packed PV cells under high concentration", *Sol. Energy.*, **85** (11), 2655 (2011).

[16] Karami, N. and Rahimi, M., "Heat transfer enhancement in a PV cell using Boehmite nanofluid", *Energy. Convers. Manage.*, **86**, 275 (2014).

[17] Khanjari, Y., Pourfayaz, F. and Kasaeian, A. B., "Numerical investigation on using of nanofluid in a water-cooled photovoltaic thermal system", *Energy. Convers. Manage.*, **122** (15), 263 (2016).

[18] Radwan, A., Ahmed, M. and Ookawara, S., "Performance enhancement of concentrated photovoltaic systems using a microchannel heat sink with nanofluids", *Energy. Convers. Manage.*, **119** (1), 289 (2016).

[19] An, W., Wu, J., Zhu, T. and Zhu, Q., "Experimental investigation of a concentrating PV/T collector with Cu9S5 nanofluid spectral splitting filter", *Appl. Energy.*, **184**, 197 (2016).

[20] Hussien, H. A., Noman, A. H. and Abdulmunem, A. R., "Indoor investigation for improving the hybrid photovoltaic/thermal system performance using nanofluid (Al_2O_3-water)", *Eng. Technol. J.*, **33** (6), 889 (2015).

[21] Al-Waeli, A. H. A., Sopian, K., Chaichan, M. T., Kazem, H. A., Hasan, H. A. and Al-Shamanim, A. N., "An experimental investigation of SiC nanofluid as a base-fluid for a photovoltaic thermal PV/T system", *Energy. Convers. Manage.*, **142**, 547 (2017).

[22] Hasan, H. A., Sopian, K., Jaaz, A. H. and Al-Shamani, A. N., "Experimental investigation of jet array nanofluids impingement in photovoltaic/thermal collector", *Sol. Energy*, **144** (1), 321 (2017).

[23] Sardarabadi, M., Passandideh-Fard, M., Maghrebi, M. J. and Ghazikhani, M., "Experimental study of using both ZnO/ water nanofluid and phase change material (PCM) in photovoltaic thermal systems", *Sol. Energy. Mater. Sol. Cells*, **161**, 62 (2017).

[24] Yazdanifard, F., Ameri, M. and Ebrahimnia-Bajestan, E., "Performance of nanofluid-based photovoltaic/thermal systems: A review", *Renew. Sustain. Energy. Reviews*, **76**, 323 (2017).

[25] Taylori, R., Coulombe, S., Otanicar, T., Phelan, P., Gunawan, A., Lv, W., Rosengarten, G., Prasher, R. and Tyagi, H., "Small particles, big impacts: A review of the diverse applications of nanofluids", *J. Appl. Phys.*, **113** (1), 11 (2013).

[26] Azimi, N., Rahimi, M. and Abdollahi. N., "Using magnetically excited

nanoparticles for liquid–liquid two-phase mass transfer enhancement in a Y-type micromixer", *Chem. Eng. Process*, **97**, 12 (2015).

[27] Azimi, N. and Rahimi, M., "Magnetic nanoparticles stimulation to enhance liquid-liquid two-phase mass transfer under static and rotating magnetic fields", *J. Magn. Magn. Mater.*, **422** (15), 188 (2017).

[28] Hajiani, P. and Larachi, F., "Ferrofluid applications in chemical engineering", *Int. Review. Chem. Eng.*, **1** (3), 221 (2009).

[29] Ghasemian M., Najafian Ashrafi, Z., Goharkhah, M. and Ashjaee, M., "Heat transfer characteristics of Fe_3O_4 ferrofluid flowing in a mini channel under constant and alternating magnetic fields", *J. Magn. Magn. Mater.*, **381** (1), 158 (2015).

[30] Chandrasekar, M., Suresh, S., Senthilkumar, T. and Ganeshkarthikeyan, M., "Passive cooling of standalone flat PV panel with cotton wick structures", *Energy. Convers. Manage.*, **71**, 43 (2013).

[31] Jang, S. H. and Shin, M. W., "Fabrication and thermal optimization of LED solar cell simulator", *Curr. Appl. Phys.*, **10** (3), 537 (2010).

[32] Li, Q. and Xuan, Y., "Experimental investigation on heat transfer characteristics of magnetic fluid flow around a fine wire under the influence of an external magnetic field", *Exp. Thermal. Fluid. Sci.*, **33** (4), 591 (2009).

[33] Lajvardi, M., Moghimi-Rad, J., Hadi, I., Gavili, A., Dallali Isfahani, T. and Zabihi, F., "Experimental investigation for enhanced ferrofluid heat transfer under magnetic field effect", *J. Magn. Magn. Mater.*, **322** (21), 3508 (2010).

[34] Ghofrani, A., Dibaei, M. H., Sima, A. H. and Shafii, M. B., "Experimental investigation on laminar forced convection heat transfer of ferrofluids under an alternating magnetic field", *Exp. Thermal. Fluid. Sci.*, **49**, 193 (2013).